0026-895X/02/6105-1124–1131
MOLECULAR PHARMACOLOGY
U.S. Government work not protected by U.S. copyright
Mol Pharmacol 61:1124–1131, 2002

Vol. 61, No. 5
1459/976854
Printed in U.S.A.

Methamphetamine Causes Coordinate Regulation of Src, Cas, Crk, and the Jun N-Terminal Kinase–Jun Pathway

SUBRAMANIAM JAYANTHI, MICHAEL T. McCOY, BRUCE LADENHEIM, and JEAN LUD CADET

Molecular Neuropsychiatry Section, Intramural Research Program, National Institutes of Health/National Institute on Drug Abuse, Baltimore, Maryland

Received October 25, 2001; accepted January 24, 2002

This article is available online at http://molpharm.aspetjournals.org

ABSTRACT

The clinical abuse of methamphetamine (METH) is a major concern because it can cause long-lasting neurodegenerative effects in humans. Current concepts of the molecular mechanisms underlying these complications have centered on the formation of reactive oxygen species. Herein, we provide cDNA microarray evidence that METH administration caused the induction of c-Jun and of other members involved in the pathway leading to c-Jun activation [stress-activated protein kinase/Jun N-terminal kinase (JNK3), Crk-associated substrate-Cas and c-Src] after environmental stresses or cytokine stimulation. Reverse transcription-polymerase chain reaction analysis confirmed these increases and also showed that the expression of JNK1 and JNK3 but not JNK2 was also increased in the METH-treated mice. Western blot analysis showed that METH increased the expression of c-Jun phosphorylated at serine-63 and serine-73 residues. Other upstream members of the JNK pathway, including phosphorylated JNKs, mitogen-activated protein kinase kinase 4, mitogen-activated protein kinase kinase 7, Crk II, Cas, and c-Src were also increased at the protein level. These values returned to baseline by 1 week after drug treatment. These results are discussed in terms of their support for a possible role of the activation of the JNK/Jun pathway in the pathophysiological effects of METH.

Methamphetamine (METH) is an illicit drug; its use has substantially increased in several regions of the United States and the world. The frequency of emergency department admissions for acute intoxication with amphetamines has also increased dramatically (Lan et al., 1998; Perez et al., 1999). These admissions are usually caused by the intake of large doses of METH, which can amount to several grams of the drug (Connell, 1958; Kramer et al., 1967). Acute intoxication with METH can be associated with acute psychosis, belligerent behaviors, or multiple organ failures, resembling clinical signs and symptoms caused by heatstroke (Lan et al., 1998). In addition, myocardial infarction, stroke, and death have been reported (Perez et al., 1999). Moreover, long-term abuse of METH can result in a paranoid-hallucinatory psychosis, which may be indistinguishable from paranoid schizophrenia (Yui et al., 1999). Reports that long-term METH abusers can also have cognitive deficits, including memory loss (Simon et al., 2000) are of significant experimental and therapeutic interest. In addition to its prolonged neurological and psychiatric effects, METH abuse may be associated with persistent neurodegenerative indices in the human brain (Ernst et al., 2000). For example, a marked reduction in striatal dopamine transporters has been demonstrated in the brains of METH abusers with the use of positron emission tomography scan (Volkow et al., 2001) and postmortem human studies (Wilson et al., 1996). This suggests that in humans, METH abuse can cause functional alterations in dopamine (DA)- (Volkow et al., 2001) and non–DA-innervated (Ernst et al., 2000) brain regions. Some of these abnormalities might be caused by large doses (0.3–1.0 g of METH taken 8–10 times daily for 3–10 days) of the drug used by some METH abusers (Connell, 1958; Kramer et al., 1967). This binge administration is followed by a crash period, which might be related in part to METH-induced monoamine depletion in various brain regions.

Studies in animals have also documented that METH can indeed cause substantial damage to various brain regions. These abnormalities include decreases in the striatal levels of DA, tyrosine hydroxylase activity, and loss of DA transporters (Cadet and Brannock, 1998). More recently, studies from our laboratory have shown that subacute administration of METH can cause apoptosis in several brain regions of mice, including the striatum, the cortex, the lateral habenula, and the hippocampus (Deng et al., 1999, 2001). These models of short-term METH injections might best represent phenomena associated with overdoses in humans, whereas

ABBREVIATIONS: METH, methamphetamine; DA, dopamine; ROS, reactive oxygen species; Src, Rous sarcoma oncogene; Cas, Crk-associated substrate; JNK, Jun N-terminal kinase; RT-PCR, reverse transcription-polymerase chain reaction; MKK4, mitogen-activated protein kinase kinase 4; MKK7, mitogen-activated protein kinase kinase 7; Crk II, avian sarcoma CT10 oncogene homolog; SAPK, stress-activated protein kinase; AP-1, activator protein 1; PLSD, protected least significant difference; ANOVA, analysis of variance.

more long-term METH injections might be more akin to the binging patterns observed in many METH abusers (Davidson et al., 2001).

Several laboratories are actively seeking to decipher the cellular and molecular mechanisms for the short- and long-term effects of the amphetamines. For example, a growing consensus suggests that reactive oxygen species (ROS) are important players in METH-induced neurodegeneration (Cadet and Brannock, 1998). Nevertheless, the complete picture of METH-induced neurodegeneration has yet to be drawn fully. It is highly likely that the dissection of intracellular signals elicited by METH-induced ROS will provide insights into the cellular and molecular cascades that are involved in the actions of this illicit stimulant. The available evidence has recently implicated the activation of immediate early genes in METH-induced damage because METH administration can cause increases in c-fos mRNA and in AP-1 DNA binding activity in mouse brain (Sheng et al., 1996b; Asanuma and Cadet, 1998). The induction in c-fos may serve a protective function because c-fos null mice showed greater severity of METH-induced apoptosis and dopaminergic toxicity (Deng et al., 1999).

Despite these observations, much remains to be done to elucidate the role of AP-1–related genes (Herdegen and Waetzig, 2001) in this model of neurodegeneration, because there is a dearth of evidence on the possible role of the c-fos binding partner, c-Jun, in the physiological or toxic effects of these illicit drugs. For example, although it has been shown that *d*-amphetamine can cause increased expression of c-Jun mRNA in rats (Persico et al., 1995) or that METH can cause activation of phosphorylated Jun kinase in the striatum (Hebert and O'Callaghan, 2000), there is a need to document whether other members of the JNK/SAPK pathway are also activated by METH.

To tackle these issues, we used the cDNA array approach to identify putative genes that might be induced by toxic doses of METH (Cadet et al., 2001). We found that METH caused an early pattern of induction of transcription factors and a delayed pattern of changes in genes related to cell death and DNA repair (Cadet et al., 2001). The changes in genes related to cell death and DNA repair could be related to METH-induced apoptosis (Deng et al., 1999, 2001). Furthermore, we had reported that several genes, including c-Jun and c-Src, were also up-regulated by the drug (Cadet et al., 2001). Because some recent observations had shown a very close relationship between ROS, Src, Cas, and JNK activation (Yoshizumi et al., 2000), we chose to test the idea that METH, which can induce ROS production (Cadet and Brannock, 1998; Jayanthi et al., 1998), might also cause the activation of molecular events similar to those reported by Yoshizumi et al. (2000). Herein, we have extended our cDNA array results (Cadet et al., 2001) by using RT-PCR and Western blot analysis and have provided a detailed time course of the effects of METH on the SAPK pathway.

Materials and Methods

Animals and Drug Treatment. Male CD-1 mice (Charles River Laboratories, Inc., Raleigh, NC) weighing 30 to 45 g were used. Mice received a single dose of 40.0 mg/kg i.p. METH or saline. Animals showed no evidence of seizures, and all the mice survived this dose regimen for the duration of the study, at least 7 days, when they were sacrificed. The single METH dose approach is an acceptable regimen that has been used by other investigators to cause marked reductions in the levels of DA, 5-hydroxytryptamine, and tyrosine hydroxylase similar to those observed with the multiple-dose schedule (Fukumura et al., 1998; Barrett et al., 2001). This approach also causes astrogliosis, which is also typical of METH toxicity (Fukumura et al., 1998). Recently, we showed that METH, given in this fashion, can cause widespread apoptosis in several brain regions (Deng et al., 2001; Jayanthi et al., 2001). The mice were sacrificed at various times after drug treatment. Brain tissues were processed for various assays as described below. All procedures involving the use of animals were according to the National Institutes of Health Guide for the Care and Use of Laboratory Animals and were approved by the local Animal Care Committee.

Probing, Hybridization, and Analysis of cDNA Arrays. cDNA array analysis was performed by using Atlas Mouse Arrays (#7741–1; BD Biosciences Clontech, Palo Alto, CA) that contain 588 cDNA segments spotted in duplicate side by side on a nylon membrane. Probing of cDNA arrays was performed as described in the BD Biosciences Clontech Atlas cDNA Expression Arrays User Manual (PT3140–1). Briefly, total RNA was isolated from the frontal cortex of saline- and METH-treated mice sacrificed 2, 4, and 16 h after the single dose of saline or METH. All tissues were placed in denaturing solution, homogenized, and extracted with phenol-chloroform by using Atlas Pure RNA Isolation Kit (BD Biosciences Clontech) and subsequently digested with DNase-I to remove any trace of DNA. After confirming the integrity of total RNA on a denaturing formaldehyde gel, 50 μg of total RNA was used as a template in a 10-μl reverse transcription reaction. A pooled set of primers complementary to the genes represented on the array (7741-1; BD Biosciences Clontech) was used for the reverse transcription probe synthesis, which was radiolabeled with ^{32}P-dATP and purified by passage over CHROMA SPIN-200 columns (BD Biosciences Clontech).

The cDNA expression array filters were prehybridized in ExpressHyb (BD Biosciences Clontech) for 30 min at 71°C and were hybridized with ^{32}P-labeled first-strand cDNA probes overnight at 71°C. After a high-stringency wash, the membranes were exposed to a PhosphorImaging screen for 24 h at room temperature. The exposed screen was scanned on a Storm 840 PhosphorImager (Molecular Dynamics, Sunnyvale, CA) at 100-μm resolution and stored as Molecular Dynamics .gel files. The array spots on the array images were analyzed using a theoretical pattern of template of Array Vision software for Windows NT (version 4; Imaging Research, St. Catherines, ON, Canada). The template elements were aligned over the true array spot, and the spot intensity value was quantified after the subtraction of set background. The signal for any given gene was calculated as the average of the signals from the two duplicate cDNA spots.

Reverse Transcription (RT)-PCR and Detection of mRNA Expression. RT-PCR with gene-specific Custom Atlas Array primers (BD Biosciences Clontech) were also used to analyze the levels of mRNAs of interest. These were carried out according to the manufacturer's protocol in both cortical and striatal tissue. RNA was extracted individually from three mice per time point. Total RNA (1 μg) was reverse-transcribed with oligo(dT) primer. For PCR amplification of cDNA, gene-specific Custom Atlas Array primers (BD Biosciences Clontech) were used to confirm changes in the levels of expression of genes of interest. The sequences for these primers are described in Table 1. The PCR reactions followed the protocol for AmpliTaq Gold (Applied Biosystems, Foster City, CA): preheating at 95°C for 10 min; repeating cycles of 95°C for 30 s, 64°C for 30 s, and 72°C for 30 s; and extending at 72°C for 7 min.

The PCR products were run on a 1.5% agarose gel at 100 V and were stained with SYBR Green (Molecular Probes, Eugene, OR). SYBR intensity in each band was measured using an IS-1000 Digital Imaging System (Alpha Innotech Corporation, San Leandro, CA) and was quantitated using FluorChem version 2.0 software (AlphaEaseFC analysis software, Alpha Innotech).

Western Blot Analysis. Analysis of c-Jun, phospho c-Jun (ser63 and ser73), JNK, and phospho JNK (New England Biolabs, Beverly, MA); phospho SEK1/MKK 4 (Cell Signaling Technology Inc., Beverly, MA); Src (Upstate Biotechnology, Lake Placid, NY); Cas (Transduction Laboratories, Lexington, KY); Crk II, MKK4, and MKK7 (SantaCruz Biotechnology Inc., Santa Cruz, CA) protein concentration in the striatum of METH-treated CD-1 mice was performed by the use of Western blot. Briefly, mice striata were homogenized in a buffer containing 320 mM sucrose, 5 mM HEPES, 1 μg/ml leupeptin, 1 μg/ml aprotinin, and 1 μg/ml pepstatin. Homogenates were centrifuged at 5000*g* for 5 min, and the supernatant fraction was subsequently centrifuged at 30,000*g* for 30 min. The resulting pellet was resuspended in the sample buffer (62.5 mM Tris-HCl, 10% glycerol, 2% SDS, 0.1% bromphenol blue, and 50 mM dithiothreitol) and subjected to SDS-polyacrylamide gel electrophoresis. Proteins were separated electrophoretically in SDS-12% polyacrylamide gels and transferred to Hybond nytran membrane. Membrane blocking, primary and secondary antibody incubations, and chemiluminescence reactions were conducted for each antibody individually according to the manufacturer's protocol. The intensity of each band was measured using an IS-1000 Digital Imaging System (Alpha Innotech) and quantitated using Flurochem version 2.0 software (AlphaEaseFC analysis software).

Statistical Analysis. Data were analyzed using statistical software (StatView 4.02; SAS Institute, Cary, NC). Statistical analysis was performed using analysis of variance (ANOVA) followed by Fisher's protected least significant difference (PLSD). The null hypothesis was rejected at the 0.05 level.

Results

METH Causes Up-Regulation of c-Jun and c-Src. The single-dose approach has recently been used to cause neurotoxic damage in rats (Fukumura et al., 1998) and neuronal cell death in several brain areas of mice (Deng et al., 2001; Jayanthi et al., 2001). Using this approach, we had performed gene expression analysis by using the mouse Atlas cDNA Array (BD Biosciences Clontech) to determine whether METH-induced adverse actions were associated with changes in specific genes that might be involved in the initiation and progression of METH-induced transcriptional effects (Cadet et al., 2001). Cluster analysis helped to identify an early pattern of up-regulation of transcription factors, including members of c-Jun family (Cadet et al., 2001), and a delayed pattern of up-regulation of genes related to cell death and DNA repair (Cadet et al., 2001; Jayanthi et al., 2001). Specifically, we found that METH caused differential regulation of several Bcl-2 family genes, which resulted in two distinct clusters consisting of up-regulation of pro-death gene expression such as Bax and down-regulation of anti-death gene expression such as Bcl-2 (Jayanthi et al., 2001). In what follows, we report further characterization of the pattern of changes observed in the c-Jun family and related genes incorporated in the array (Cadet et al., 2001) by providing RT-PCR confirmation and extension of the time course of these changes. We also provide detailed measurements of proteins encoded by these genes. As stated above, we chose to do so because the JNK/SAPK pathway has been implicated in several models of neurotoxic processes in the central nervous system (Herdegen and Waetzig, 2001).

A cDNA array analysis showed that c-Jun and other genes potentially involved in c-Jun activation (JNK3, Cas, and Src) were induced by METH treatment (Cadet et al., 2001). Figure 1A shows that there was little variability between transcript levels measured by duplicate spots corresponding to a given gene ($r^2 = 0.951, p < 0.0001$). The increased expression of the genes of interest found on the BD Biosciences Clontech array (#7741–1) was confirmed by RT-PCR analysis (Fig. 1B). Because of the possible involvement of the AP-1 family of genes in METH neurotoxicity (Sheng et al., 1996b; Deng et al., 1999) and of the reported participation of the JNK/SAPK pathway in neuronal apoptosis (Herdegen et al., 1998; Watson et al., 1998), we chose to further characterize the JNK cascade in this model by using RT-PCR and Western blot analyses while extending the time course of observations.

RT-PCR Evidence for METH-Induced Increased Transcript Levels for Downstream and Upstream Members of the JNK/SAPK Cascade in the Cortex and the Striatum. Figure 2 shows a representative RT-PCR photomicrograph of METH-mediated induction in the expression of members located downstream and upstream of JNK in the JNK/SAPK pathway in the cortex. The quantification of the RT-PCR changes is provided in Fig. 3, A through D and E through H, for the cortex and the striatum, respectively. Although only JNK3 was incorporated in the BD Biosciences Clontech array (#7741–1) used in our array experiments (Cadet et al., 2001), we also ran RT-PCR of two other isoforms of JNKs, namely JNK1 and JNK2 (Figs. 2, 3C, and 3F). Expression of JNK1 and JNK3 but not JNK2 transcripts was higher in METH-treated mice compared with saline-treated mice (Figs. 2 and 3C). In the frontal cortex (Fig. 3, A through D), the increases in the expression of the various members of JNK cascade peaked at 8 h. In contrast, Fig. 3, E through H, showed that the METH induction up-regulation of these transcripts in the mouse striatum occurred somewhat earlier (2–4 h) than did those observed in the cortex (8 h) (compare Fig. 3, A through D, with Fig. 3, E through H, respectively).

METH Causes Increases in Protein Levels and in Protein Phosphorylation of Members of the JNK/SAPK Pathway in the Striatum. MAP kinase cascades are believed to be among the most important intracellular signaling pathways transmitting signals from the cell membrane to the nucleus, and their most prominent function is believed to be the regulation of cellular gene expression via phosphory-

TABLE 1
Primer sequences

Gene of Interest	No. of Cycles Used	Upstream Primer	Downstream Primer
c-Jun	30	ATGCCCTCAACGCCTCGTTCCTCC	CTGCTCGTCGGTCACGTTCTTGGG
JNK1	30	TGTGGAATCAAGCACCTTCACTCTGCTG	GCAAACCATTTCTCCCATAATGCACCC
JNK2	30	CTAGGAACACCATCCGCAGAGTTC	GCTTCGTCCACAGAGATCCGCTTG
JNK3	30	CCACGAGCGGATGTCTTACTTGC	TTGTAGCCCATGCCCAGGATGACC
MKK7	29	TGAACAAGGTTGATGGGAGCC	AGCCAAGCTGAAGCAGGAGAA
MKK4	28	TGGACAGCTTGTGGACTCTATTGC	CTGGCATCTGATCCAGGATTTTAC
Cas	28	GTTCACCTCCCAGGACTCTCC	GCCAGGTCGTGGTCTATTGGACG
Src	28	GGGCAACAAAGTTGCAGTCAAGTGC	GCCACGTTGTCTTCAGACACCAGC

lation of transcription factors (Fukunaga and Miyamoto, 1998). c-Jun activity is regulated via phosphorylation at serines 63 and 73 located in its activation domain. This is mediated by members of JNK/SAPKs family, namely JNK1, JNK2, and JNK3 (Derijard et al., 1994). Phosphorylation of c-Jun potentiates its ability to activate the transcription of AP1 target genes (Herdegen and Waetzig, 2001).

To determine whether the METH-induced increases in transcript levels of members of the JNK cascade were also accompanied by changes in protein levels and in their phosphorylation states, we performed an immunoblot analysis using available antibodies specific for the phosphorylated forms of c-Jun, JNK, and MKK4. To accomplish that end, we used a Western blot analysis and carried a more detailed time course of protein expression in the striata of mice treated with METH (Figs. 4 and 5, A through D). Striatal tissue was chosen for further investigations of protein expression because the striatum is markedly affected by METH administration (Wilson et al., 1996; Deng et al., 1999; Volkow et al., 2001). Moreover, DA-induced cell death, both in vivo (Luo et al., 1999a) and in vitro (Luo et al., 1998, 1999b), seems to occur via activation of the JNK pathway. Figure 5D shows that there was an almost immediate increase in c-Jun protein after the METH injection. These changes were first observed at 15 min ($p < 0.01$), peaked at 4 h ($p < 0.001$), and then returned to basal level by 7 days ($p < 0.05$) after drug administration. Phosphorylation of c-Jun at ser73 was very intense from 4 to 16 h ($p < 0.001$), whereas phosphorylation at ser63 was greatest approximately 2 to 4 h ($p < 0.001$) after METH treatment (Fig. 5D).

Because the phosphorylation of c-Jun is mediated by the JNKs, we also measured the levels of these proteins and their phosphorylation states using Western blot analysis. As shown in Fig. 5C, there were also METH-induced increases in JNK protein expression in mice striata. JNK protein expression increased with time and then showed a pattern that was somewhat similar to that observed for phosphorylated c-Jun (compare Fig. 5C with 5D). Two bands were observed,

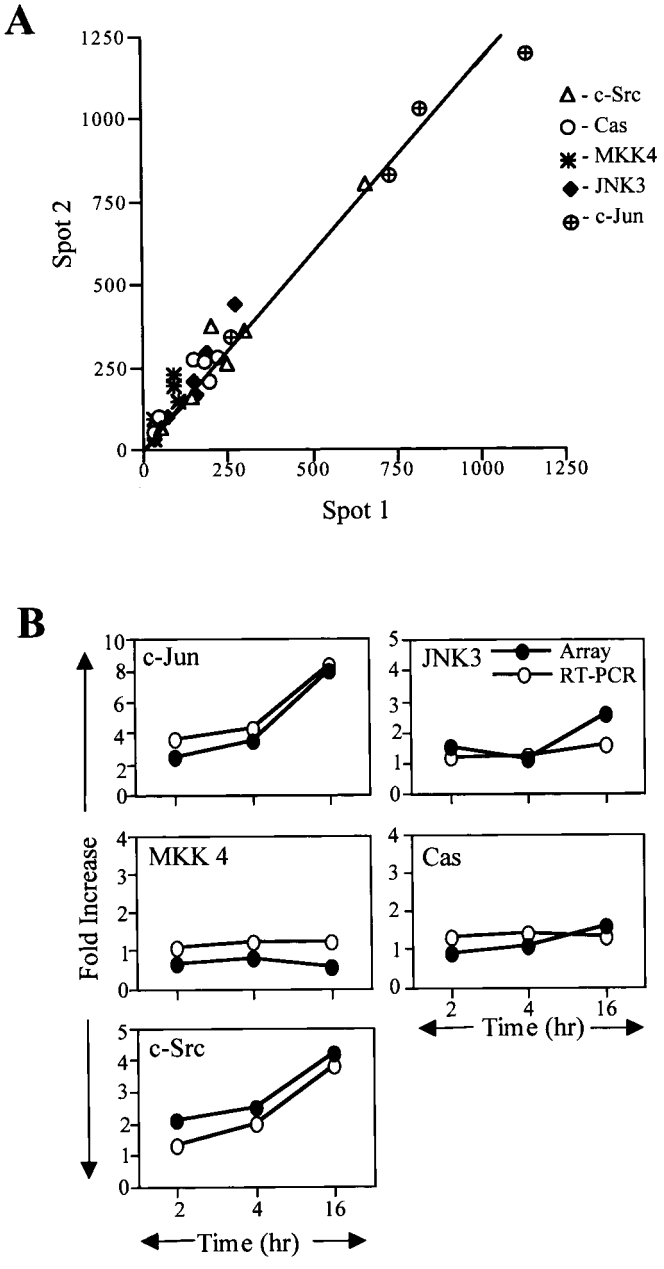

Fig. 1. A, scatter plot of duplicate spots representing a single gene on the mouse cDNA expression array (#7741–1). The genes represented include c-Jun, JNK3, MKK4, Cas, and Src. There was a significant linear correlation ($r^2 = 0.951$; $p < 0.0001$) between the intensity measured for the two duplicate spots on the array. B, RT-PCR confirmation of METH-induced changes in gene expression observed in the cDNA array analysis. The changes in gene expression profiles were similar between the two analyses. The data for the RT-PCR were obtained from triplicate determinations, whereas those for the cDNA array were done in duplicates.

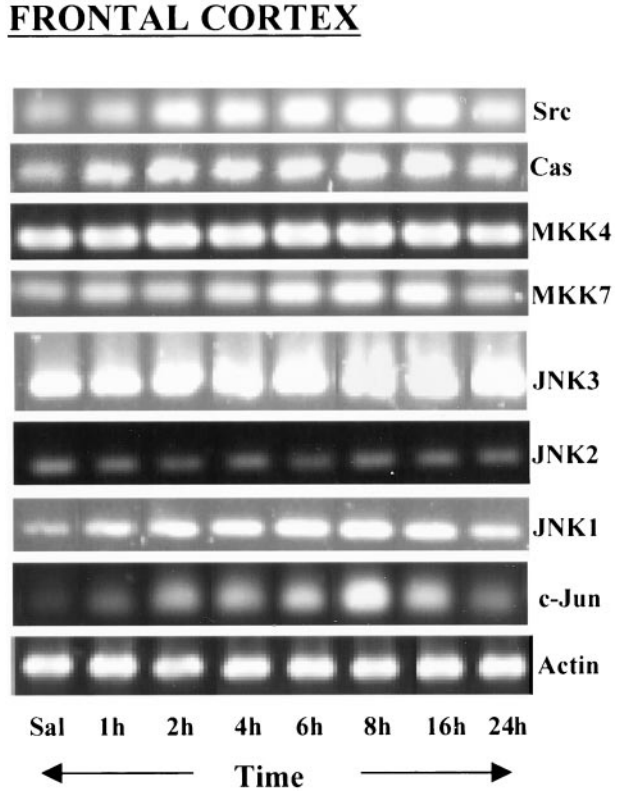

Fig. 2. Representative photomicrograph of RT-PCR results showing the effects of METH on the transcript levels of members of the SAPK/JNK in the mouse neocortex. RNA was obtained from the cortices of saline-and METH-treated CD-1 mice. Mice were sacrificed at the various times listed after the METH injections. RT-PCR was performed as described in under *Materials and Methods*. β-Actin is included as a control and shows no changes during the course of the experiments.

one at 46 kDa and another at 54 kDa, with increases observed in both bands (2–48 h; $p < 0.001$). Similar changes in JNK expression had previously been reported after intracerebral injections of ibotenic acid in the rat (Ferrer et al., 1997b) or after transient forebrain ischemia in the gerbil (Ferrer et al., 1997a). Because the activity of JNK is increased after their phosphorylation at threonine 183 and tyrosine 185 (Tournier et al., 1997), we also sought to determine whether there were any changes in JNK phosphorylation after METH treatment. Figure 5C also shows that there was indeed a substantial increase in the phosphorylation of the p46 and p54 bands ($p < 0.001$). According to the manufacturer's literature (New England Biolabs), the antibody against phospho-JNK recognizes the dually phosphorylated isoforms of JNK1, JNK2, and JNK3.

Western blot analysis was also used to characterize more upstream members of the JNK pathway (Fig. 5, A and B). The SH2 and SH3 domains of Crk II have been shown to bind to JNK (Yoshizumi et al., 2000) and to activate it via the tyrosine-phosphorylated effector molecule, Cas. Alternatively, JNK activation is accomplished upon its phosphorylation by upstream kinases, MKK4 (Derijard et al., 1995) or MKK7 (Moriguchi et al., 1997). As shown in Figs. 4 and 5A, c-Src, Cas, and Crk II showed increases after treatment with METH and returned to basal levels after 1 week. MKK4, also known as MEK4, showed an increase at the 4-h time point ($p < 0.05$, Fig. 5B). MKK4 did not show any significant increases in its phosphorylated state after METH treatment (Fig. 5B). In contrast, MKK7 showed significant increases from the 1-h time point ($p < 0.001$), with subsequent slow reversal to normal over a 7-day period (Fig. 5B).

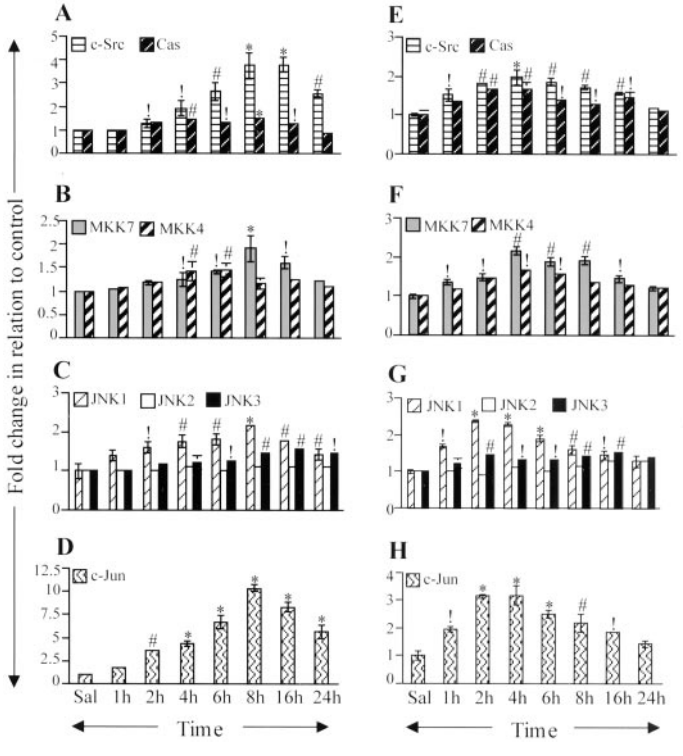

Fig. 3. Quantitative rendering of the RT-PCR data obtained from the frontal cortex (A through D) and the striatum (E through H). Upstream (A, B, E, and F) and downstream (C, D, G, and H) members of the SAPK/JNK pathway are shown. The values represent means ± S.E.M. obtained from three mice per time point. The fold changes on the *y*-axis were generated in comparison to saline-injected animals. The times on the *x*-axis represent time points after drug injections. Statistical analysis was performed using one-way ANOVA, followed by Fisher's PLSD. !, $p < 0.05$; #, $p < 0.01$, and *, $p < 0.001$ compared with saline-injected mice.

Discussion

The major findings of our study show that METH-induced c-Jun expression is associated with JNK-induced c-Jun phosphorylation and that JNK activation occurs via stimulation of the Src-Cas-Crk upstream pathway. We discuss the possible involvement of that pathway in the pathobiological events associated with the use of METH from the wealth of information that links that pathway to a number of pathobiological states (Herdegen and Waetzig, 2001).

Possible Mechanisms for METH-Induced Activation of the JNK Pathway. In this study, we found that a single injection of METH can cause increases in the levels of c-Jun mRNA and its protein in the mouse brain. These findings extend those of Persico et al. (1995), who reported that *d*-amphetamine can cause increases in c-Jun mRNA in rats. Because the ability of c-Jun to activate gene transcription is potentiated by phosphorylation at serine residues 63 and 73 of the c-Jun activation domain (Derijard et al., 1994), the increase in phosphorylated ser63 and ser73 c-Jun observed after METH administration may be of significance to METH-induced cellular damage. This idea is supported by the observations of increases in c-Jun phosphorylated at ser63 in models of neuronal death caused by trophic factor withdrawal (Watson et al., 1998) and by the report of an involvement of c-Jun phosphorylated at ser73 in ischemia-induced neuronal damage (Herdegen et al., 1998).

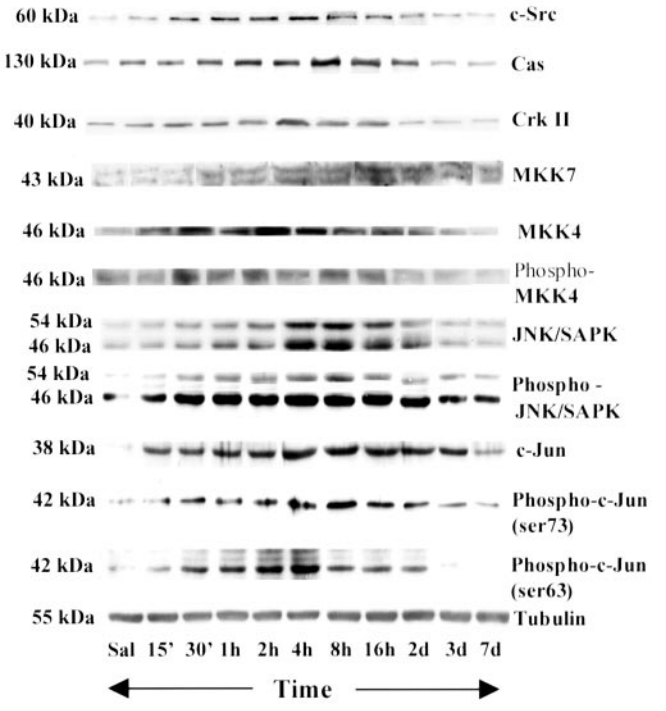

Fig. 4. Representative photomicrograph of results showing the effects of METH on the protein levels of members of the SAPK/JNK in the striatal tissue of mice at different time points after the administration of METH. Pooled protein samples from five mice per time point were used for the Western blots, and the experiments were repeated three times. The quantification of those data is provided in Fig. 5. Tubulin is included as a control and shows no changes during the course of the experiments.

It is also of interest that METH administration caused differential responses in the time course activation of the three JNKs. Specifically, JNK1 mRNA showed a steady increase with time, peaked at 8 h, and then showed a downward trend. JNK3 mRNA showed a gradual increase and remained elevated even at 24 h, whereas JNK2 mRNA showed no significant changes. These results suggest that METH-induced c-Jun phosphorylation, which occurred very early and lasts for a while, might depend on both the early JNK1 expression and the somewhat delayed activation of JNK3. This suggestion is supported by the observation that

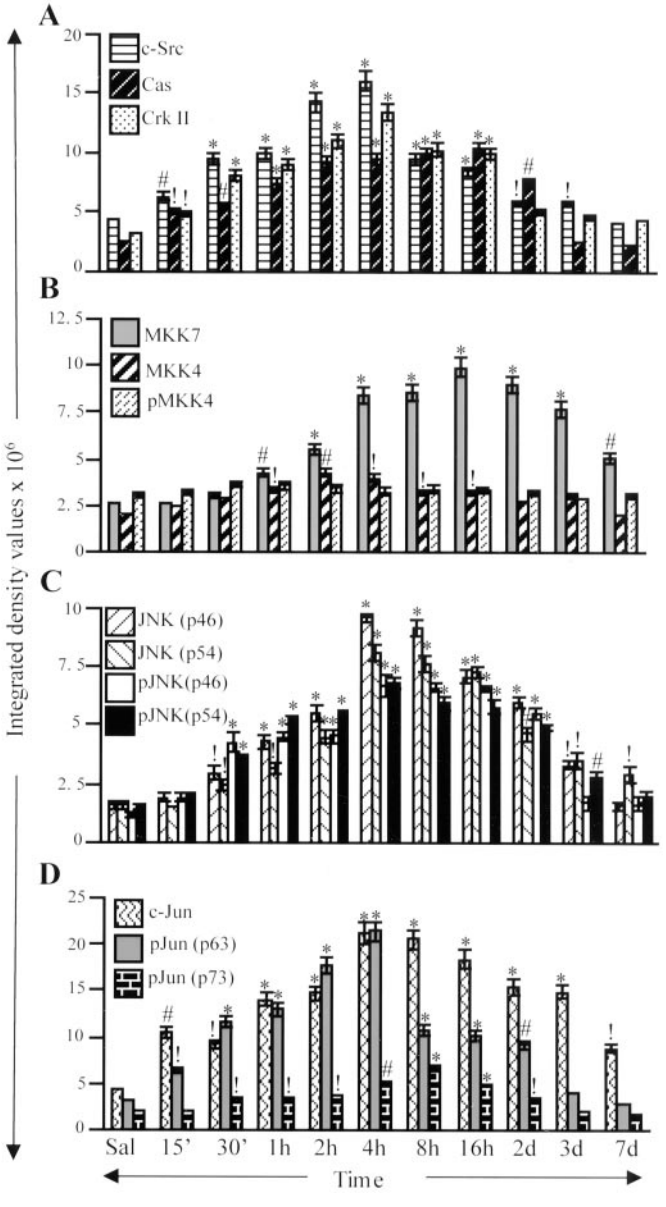

Fig. 5. Quantification of the Western blot data obtained from the striatum. METH-induced changes in upstream (A, B) and downstream (C, D) members of the JNK/SAPK pathway are shown. The values represent the mean ± S.E.M. data obtained from three experiments. The density of each band was calculated as an integrated density value using AlphaEaseFC analysis software (IS-1000 Digital Imaging System). Integrated density value is the sum of all pixel values obtained after background correction. Statistical analysis was performed using one-way ANOVA followed by PLSD. !, $p < 0.05$; #, $p < 0.01$, and *, $p < 0.001$ compared with saline-injected mice.

although JNK1, JNK2, and JNK3 protein kinases all mediate the phosphorylation of c-Jun at ser63 and ser73 in response to external stress signals, they seem to have stimulus-specific biological functions (Mielke et al., 2000). For example, JNK1 and JNK2 are widely expressed in most cell types (Mielke et al., 2000), whereas JNK3 is mainly expressed in the nervous system (Gupta et al., 1996). Moreover, Jun-JNK complexes formed in response to tumor necrosis factor seem to consist mostly of JNK1-c-Jun instead of JNK2-c-Jun (Zhang et al., 1998). In any case, given the observations that JNK seems to be involved in several models of neuronal death (Herdegen et al., 1998; Watson et al., 1998), it is not farfetched to suggest that the METH-induced increases in phosphorylated c-Jun and its kinases might play important roles in METH-induced apoptotic events (Deng et al., 2001). This suggestion is supported by observations that JNK3 null mice are resistant to kainate-induced cell death (Yang et al., 1997) and by our recent demonstration that c-Jun knockout mice are protected against METH-induced apoptosis (unpublished observations). Other central nervous system active drugs such as morphine (Fuchs and Pruett, 1993) and haloperidol (Noh et al., 2000), which can cause apoptosis, have also been reported to activate the JNK pathway (Noh et al., 2000; Ma et al., 2001).

The manner by which METH might cause activation of the JNKs is not clear. However, our results showing that c-Src mRNA and protein expression increased proportionally with c-Jun and JNK expression suggest that METH might mediate JNK activation via Src because Src can stimulate JNK activity (Feng et al., 2001). This is supported by the recent demonstration that adenoviral transfection of a dominant-negative form of Src can abrogate H_2O_2-induced JNK activation (Chen et al., 2001). Src-dependent signal events are mediated by the assembly of signal transduction complex that involves Cas and Crk via SH2 binding motifs (Burnham et al., 1996). Cas is the major tyrosine-phosphorylated protein in cells transformed by Src (Sakai et al., 1994). The unique structure of this protein, with amino-terminal SH3 domain, followed by a cluster of SH2 binding motifs and a carboxyl-terminal domain containing Src SH3 and SH2 binding regions, provides an important scaffold for the assembly of a multiprotein signaling complex (Sakai et al., 1994). Thus, our observations of proportional increases in Cas and Crk protein expression in conjunction with Src suggest that such an assembly may mediate Src-dependent signaling events. Recent studies by Yoshizumi et al. (2000) in H_2O_2-treated cells have indeed demonstrated Src-dependent Cas tyrosine phosphorylation, Cas-Crk complex formation, and binding of the SH3 domain of Crk to JNK with associated activation of JNK. Taken together, these observations suggest a novel redox-sensitive pathway for METH-induced JNK activation.

JNK activation can also be accomplished via its phosphorylation by upstream kinases MKK4 (Derijard et al., 1995) or MKK7 (Tournier et al., 1997). Ward and Hagg (2000) showed a disjunction between the activation patterns of MKK4 and c-Jun during injury by reporting the presence of c-Jun phosphorylation in the absence of MKK4 phosphorylation. In the present study, we failed to detect substantial increases in phospho-MKK4 even though there was prominent METH-induced c-Jun phosphorylation. These results suggest that MKK7 might be a more important factor in METH-induced JNK activation. Nevertheless, given the long time course of

the increases observed in MKK7 and the similar time-course of METH-induced phosphorylated JNKs, our results suggest that the Src-Cas-Crk connection via activation of MKK7 might play a very prominent role in the prolonged JNK phosphorylation.

Possible Relationships between METH, Oxidative Stress, and JNK Activation. As stated earlier, the long-term deleterious effects of amphetamine analogs are believed to be related to increased production of ROS (Cadet and Brannock, 1998; Jayanthi et al., 1998). This is believed to occur via increased METH-induced release of dopamine within DA terminals or in the synaptic cleft, with subsequent formation of quinone, superoxide anions, H_2O_2, and hydroxyl radicals (Cadet and Brannock, 1998). These DA-associated reactive species might act in concert to cause the induction and phosphorylation of c-Jun via activation of JNK/SAPKs (Fei et al., 2000). This idea is supported by recent reports that DA can cause activation of the JNK pathway both in vitro (Luo et al., 1998) and in vivo (Luo et al., 1999a). These suggestions are supported by reports that JNK activation paralleled the course of ROS formation in endothelin-stimulated smooth muscle cells (Fei et al., 2000). Further support for this notion is also provided by the observations that the superoxide generator menadione and H_2O_2 can activate the Src-dependent JNK pathway (Yoshizumi et al., 2000; Chen et al., 2001). Similar observations have been made with other agents that cause oxidative stress (Verheij et al., 1996) and agents that can cause oxidative injury by depleting cellular glutathione (Wilhelm et al., 1997).

It is important to point out that in addition to causing DA release and production of ROS, METH can also induce a marked increase in synaptic glutamate in the rodent striatum (Stephans and Yamamoto, 1994). The released glutamate could activate glutamate receptors with subsequent changes in intracellular calcium and secondary increases in the production of the physiological regulator nitric oxide (Radi et al., 1991). Thus, METH administration might also activate the JNK pathway via the actions of glutamate on striatal cells, as demonstrated by Schwarzschild et al. (1997) using primary cultures of the striatum. This idea is consistent with the demonstration that nitric oxide is involved in the neurodegenerative effects of METH (Sheng et al., 1996a).

Summary

In summary, administration of a single moderate dose of METH caused persistent JNK activation with increases in c-Jun expression and phosphorylation. These results hint to the possibility that METH-induced DA and glutamate release, with subsequent ROS and nitric oxide production, might work in concert to activate the Src-JNK-Jun cascade. Activation of this cascade could then lead to increases in the expression of Jun effector genes that might be involved in causing neurodegeneration. In any case, the identification of c-Jun target genes should provide substantial insights into the molecular neurotoxicology of this stimulant. These studies are underway in our laboratory.

References

Asanuma M and Cadet JL (1998) Methamphetamine-induced increase in striatal NF-kappaB DNA-binding activity is attenuated in superoxide dismutase transgenic mice. *Brain Res Mol Brain Res* **60:**305–309.

Barrett T, Xie T, Piao Y, Dillon-Carter O, Kargul GJ, Lim MK, Chrest FJ, Wersto R, Rowley DL, Juhaszova M, et al. (2001) A murine dopamine neuron-specific cDNA library and microarray increased COXI expression during methamphetamine neurotoxicity. *Neurobiol Dis* **8:**822–833.

Burnham MR, Harte MT, Richardson A, Parsons JT, and Bouton AH (1996) The identification of p130cas-binding proteins and their role in cellular transformation. *Oncogene* **12:**2467–2472.

Cadet JL and Brannock C (1998) Free radicals and the pathobiology of brain dopamine systems. *Neurochem Int* **32:**117–131.

Cadet JL, Jayanthi S, McCoy MT, Vawter M, and Ladenheim B (2001) Temporal profiling of methamphetamine-induced changes in gene expression in the mouse brain: evidence from cDNA array. *Synapse* **41:**40–48.

Chen K, Vita JA, Berk BC, and Keaney JF Jr (2001) c-Jun N-terminal kinase activation by hydrogen peroxide in endothelial cells involves src-dependent epidermal growth factor receptor transactivation. *J Biol Chem* **276:**16045–16050.

Connell PH (1958) *Amphetamine Psychosis*, Oxford University Press, London.

Davidson C, Gow AJ, Lee TH, and Ellinwood EH (2001) Methamphetamine neurotoxicity: necrotic and apoptotic mechanisms and relevance to human abuse and treatment. *Brain Res Brain Res Rev* **36:**1–22.

Deng X, Ladenheim B, Tsao LI, and Cadet JL (1999) Null mutation of c-fos causes exacerbation of methamphetamine-induced neurotoxicity. *J Neurosci* **19:**10107–10115.

Deng X, Wang Y, Chou J, and Cadet JL (2001) Methamphetamine causes widespread apoptosis in the mouse brain: evidence from using an improved TUNEL histochemical method. *Brain Res Mol Brain Res* **93:**64–69.

Derijard B, Hibi M, Wu IH, Barrett T, Su B, Deng T, Karin M, and Davis RJ (1994) JNK1: a protein kinase stimulated by UV light and Ha-Ras that binds and phosphorylates the c-Jun activation domain. *Cell* **76:**1025–1037.

Derijard B, Raingeaud J, Barrett T, Wu IH, Han J, Ulevitch RJ, and Davis RJ (1995) Independent human MAP-kinase signal transduction pathways defined by MEK and MKK isoforms. *Science(Wash DC)* **267:**682–685.

Ernst T, Chang L, Leonido-Yee M, and Speck O (2000) Evidence for long-term neurotoxicity associated with methamphetamine abuse: a 1H MRS study. *Neurology* **54:**1344–1349.

Fei J, Viedt C, Soto U, Elsing C, Jahn L, and Kreuzer J (2000) Endothelin-1 and smooth muscle cells: induction of jun amino-terminal kinase through an oxygen radical-sensitive mechanism. *Arterioscler Thromb Vasc Biol* **20:**1244–1249.

Feng W, Webb P, Nguyen P, Liu X, Li J, Karin M, and Kushner PJ (2001) Potentiation of estrogen receptor activation function 1 (AF-1) by Src/JNK through a serine 118-independent pathway. *Mol Endocrinol* **15:**32–45.

Ferrer I, Ballabriga J, and Pozas E (1997a) Transient forebrain ischemia in the adult gerbil is associated with a complex c-Jun response. *Neuroreport* **8:**2483–2487.

Ferrer I, Pozas E, Ballabriga J, and Planas AM (1997b) Strong c-Jun/AP-1 immunoreactivity is restricted to apoptotic cells following intracerebral ibotenic acid injection in developing rats. *Neurosci Res* **28:**21–31.

Fuchs BA and Pruett SB (1993) Morphine induces apoptosis in murine thymocytes in vivo but not in vitro: involvement of both opiate and glucocorticoid receptors. *J Pharmacol Exp Ther* **266:**417–423.

Fukumura M, Cappon GD, Pu C, Broening HW, and Vorhees CV (1998) A single dose model of methamphetamine-induced neurotoxicity in rats: effects on neostriatal monoamines and glial fibrillary acidic protein. *Brain Res* **806:**1–7.

Fukunaga K and Miyamoto E (1998) Role of MAP kinase in neurons. *Mol Neurobiol* **16:**79–95.

Gupta S, Barrett T, Whitmarsh AJ, Cavanagh J, Sluss HK, Derijard B, and Davis RJ (1996) Selective interaction of JNK protein kinase isoforms with transcription factors. *EMBO (Eur Mol Biol Organ) J* **15:**2760–2770.

Hebert MA and O'Callaghan JP (2000) Protein phosphorylation cascades associated with methamphetamine- induced glial activation. *Ann NY Acad Sci* **914:**238–262.

Herdegen T, Claret FX, Kallunki T, Martin-Villalba A, Winter C, Hunter T, and Karin M (1998) Lasting N-terminal phosphorylation of c-Jun and activation of c-Jun N- terminal kinases after neuronal injury. *J Neurosci* **18:**5124–5135.

Herdegen T and Waetzig V (2001) AP-1 proteins in the adult brain: facts and fiction about effectors of neuroprotection and neurodegeneration. *Oncogene* **20:**2424–2437.

Jayanthi S, Deng X, Boredelon M, McCoy MT, and Cadet JL (2001) Methamphetamine causes differential regulation of pro-death and anti-death Bcl-2 genes in the mouse neocortex. *FASEB J* **15:**1745–1752.

Jayanthi S, Ladenheim B, and Cadet JL (1998) Methamphetamine-induced changes in antioxidant enzymes and lipid peroxidation in copper/zinc-superoxide dismutase transgenic mice. *Ann NY Acad Sci* **844:**92–102.

Kramer JC, Fischman VS, and Littlefield DC (1967) Amphetamine abuse. Pattern and effects of high doses taken intravenously. *JAMA* **201:**305–309.

Lan KC, Lin YF, Yu FC, Lin CS, and Chu P (1998) Clinical manifestations and prognostic features of acute methamphetamine intoxication. *J Formos Med Assoc* **97:**528–533.

Luo Y, Hattori A, Munoz J, Qin ZH, and Roth GS (1999a) Intrastriatal dopamine injection induces apoptosis through oxidation- involved activation of transcription factors AP-1 and NF-kappaB in rats. *Mol Pharmacol* **56:**254–264.

Luo Y, Kokkonen GC, Hattori A, Chrest FJ, and Roth GS (1999b) Dopamine stimulates redox-tyrosine kinase signaling and p38 MAPK in activation of astrocytic C6–D2L cells. *Brain Res* **850:**21–38.

Luo Y, Umegaki H, Wang X, Abe R, and Roth GS (1998) Dopamine induces apoptosis through an oxidation-involved SAPK/JNK activation pathway. *J Biol Chem* **273:**3756–3764.

Ma W, Zheng WH, Powell K, Jhamandas K, and Quirion R (2001) Chronic morphine exposure increases the phosphorylation of MAP kinases and the transcription factor CREB in dorsal root ganglion neurons: an in vitro and in vivo study. *Eur J Neurosci* **14:**1091–1104.

Mielke K, Damm A, Yang DD, and Herdegen T (2000) Selective expression of JNK isoforms and stress-specific JNK activity in different neural cell lines. *Brain Res Mol Brain Res* **75:**128–137.

Moriguchi T, Toyoshima F, Masuyama N, Hanafusa H, Gotoh Y, and Nishida E

(1997) A novel SAPK/JNK kinase, MKK7, stimulated by TNFalpha and cellular stresses. *EMBO (Eur Mol Biol Organ) J* **16:**7045–7053.
Noh JS, Kang HJ, Kim EY, Sohn S, Chung YK, Kim SU, and Gwag BJ (2000) Haloperidol-induced neuronal apoptosis: role of p38 and c-Jun-NH(2)-terminal protein kinase. *J Neurochem* **75:**2327–2334.
Perez JA Jr, Arsura EL, and Strategos S (1999) Methamphetamine-related stroke: four cases. *J Emerg Med* **17:**469–471.
Persico AM, Schindler CW, Zaczek R, Brannock MT, and Uhl GR (1995) Brain transcription factor gene expression, neurotransmitter levels, and novelty response behaviors: alterations during rat amphetamine withdrawal and following chronic injection stress. *Synapse* **19:**212–227.
Radi R, Beckman JS, Bush KM, and Freeman BA (1991) Peroxynitrite-induced membrane lipid peroxidation: the cytotoxic potential of superoxide and nitric oxide. *Arch Biochem Biophys* **288:**481–487.
Sakai R, Iwamatsu A, Hirano N, Ogawa S, Tanaka T, Mano H, Yazaki Y, and Hirai H (1994) A novel signaling molecule, p130, forms stable complexes in vivo with v-Crk and v-Src in a tyrosine phosphorylation-dependent manner. *EMBO (Eur Mol Biol Organ) J* **13:**3748–3756.
Schwarzschild MA, Cole RL, and Hyman SE (1997) Glutamate, but not dopamine, stimulates stress-activated protein kinase and AP-1-mediated transcription in striatal neurons. *J Neurosci* **17:**3455–3466.
Sheng P, Cerruti C, Ali S, and Cadet JL (1996a) Nitric oxide is a mediator of methamphetamine (METH)-induced neurotoxicity. In vitro evidence from primary cultures of mesencephalic cells. *Ann NY Acad Sci* **801:**174–186.
Sheng P, Wang XB, Ladenheim B, Epstein C, and Cadet JL (1996b) AP-1 DNA-binding activation by methamphetamine involves oxidative stress. *Synapse* **24:**213–217.
Simon SL, Domier C, Carnell J, Brethen P, Rawson R, and Ling W (2000) Cognitive impairment in individuals currently using methamphetamine. *Am J Addict* **9:**222–231.
Stephans SE and Yamamoto BK (1994) Methamphetamine-induced neurotoxicity: roles for glutamate and dopamine efflux. *Synapse* **17:**203–209.
Tournier C, Whitmarsh AJ, Cavanagh J, Barrett T, and Davis RJ (1997) Mitogen-activated protein kinase kinase 7 is an activator of the c-Jun NH2-terminal kinase. *Proc Natl Acad Sci USA* **94:**7337–7342.
Verheij M, Bose R, Lin XH, Yao B, Jarvis WD, Grant S, Birrer MJ, Szabo E, Zon LI, Kyriakis JM, et al. (1996) Requirement for ceramide-initiated SAPK/JNK signalling in stress- induced apoptosis. *Nature (Lond)* **380:**75–79.
Volkow ND, Chang L, Wang GJ, Fowler JS, Leonido-Yee M, Franceschi D, Sedler MJ, Gatley SJ, Hitzemann R, Ding YS, et al. (2001) Association of dopamine transporter reduction with psychomotor impairment in methamphetamine abusers. *Am J Psychiatry* **158:**377–382.
Ward NL and Hagg T (2000) SEK1/MKK4, c-Jun and NFKappaB are differentially activated in forebrain neurons during postnatal development and injury in both control and p75NGFR-deficient mice. *Eur J Neurosci* **12:**1867–1881.
Watson A, Eilers A, Lallemand D, Kyriakis J, Rubin LL, and Ham J (1998) Phosphorylation of c-Jun is necessary for apoptosis induced by survival signal withdrawal in cerebellar granule neurons. *J Neurosci* **18:**751–762.
Wilhelm D, Bender K, Knebel A, and Angel P (1997) The level of intracellular glutathione is a key regulator for the induction of stress-activated signal transduction pathways including Jun N-terminal protein kinases and p38 kinase by alkylating agents. *Mol Cell Biol* **17:**4792–4800.
Wilson JM, Kalasinsky KS, Levey AI, Bergeron C, Reiber G, Anthony RM, Schmunk GA, Shannak K, Haycock JW, and Kish SJ (1996) Striatal dopamine nerve terminal markers in human, chronic methamphetamine users. *Nat Med* **2:**699–703.
Yang DD, Kuan CY, Whitmarsh AJ, Rincon M, Zheng TS, Davis RJ, Rakic P, and Flavell RA (1997) Absence of excitotoxicity-induced apoptosis in the hippocampus of mice lacking the Jnk3 gene. *Nature (Lond)* **389:**865–870.
Yoshizumi M, Abe J, Haendeler J, Huang Q, and Berk BC (2000) Src and Cas mediate JNK activation but not ERK1/2 and p38 kinases by reactive oxygen species. *J Biol Chem* **275:**11706–11712.
Yui K, Goto K, Ikemoto S, Ishiguro T, Angrist B, Duncan GE, Sheitman BB, Lieberman JA, Bracha SH, and Ali SF (1999) Neurobiological basis of relapse prediction in stimulant-induced psychosis and schizophrenia: the role of sensitization. *Mol Psychiatry* **4:**512–523.
Zhang P, Hogan EL, and Bhat NR (1998) Activation of JNK/SAPK in primary glial cultures: II. Differential activation of kinase isoforms corresponds to their differential expression. *Neurochem Res* **23:**219–225.

Address correspondence to: Jean Lud Cadet, M.D., Molecular Neuropsychiatry Section, NIH/NIDA Intramural Research Program, 5500 Nathan Shock Drive, Baltimore, MD 21224. E-mail: jcadet@intra.nida.nih.gov